

# Propagation of Ultra-High Energy Cosmic Rays in Extragalactic Magnetic Fields

Tadeusz Wibig<sup>1,2</sup> \*

<sup>1</sup> *Experimental Physics Department,  
University of Łódź  
Pomorska 149/153, 90-236 Łódź*

<sup>2</sup> *The Andrzej Soltan Institute For Nuclear Studies,  
Cosmic Ray Laboratory  
Uniwersytecka 5, POB 447, 90-950 Łódź 1, Poland*

Received 23 December 2003; accepted 21 February 2004

---

**Abstract:** In this paper we will discuss the problem of Ultra High Energy Cosmic Rays (UHECR) and show that the idea of a Single Source Model established by Erlykin and Wolfendale (1997) to explain the features seen in cosmic ray energy spectra around the  $10^{15}$  eV region can be successfully applied also for the much higher energies. The propagation of UHECR (of energies higher than  $10^{19}$  eV) in extragalactic magnetic fields can no longer be described as a random walk (diffusion) process and the transition to rectilinear propagation gives a possible explanation for the so-called Greisen-Zatsepin-Kuzmin (GZK) cut-off which still remains an open question after almost 40 years. A transient “single source” located at a particular distance and producing UHECR for a finite time is the proposed solution.

© Central European Science Journals. All rights reserved.

*Keywords: cosmic rays, CR sources and composition, CR anisotropy*  
*PACS (2000): 95.85.Ry, 96.40.De, 96.40.Pq*

---

## 1 Introduction

The phenomenon known as cosmic rays, and particularly the observed flux of particles of extremely high energies, is a perfect example of the situation where the subject of study is “one and only” in nature – *i.e.*, we only have one set of data. Thus, in trying to explain it, one does not have to rely on the “most probable” or “average” solution. The phenomenon as we see it, here and now, could be the result of a particular chain of

---

\* E-mail: wibig@zpk.u.lodz.pl

coincidences. If this chain is not “very improbable,” it may just be the right solution.

This concept was used by Erlykin and Wolfendale a few years ago [1] in the Single Source Model (SSM) of CR origin. Originally it was established to explain the shape of the so-called “knee” in the CR energy spectrum seen in many experiments over a period of almost 50 years. Careful analysis of very accurate data on Extensive Air Showers collected by different experiments made in [2] shows the existence of sharp structures around the estimated primary CR particle energy of a few times  $10^{15}$  eV. In subsequent papers by Erlykin and Wolfendale [3], it was shown that the Single Source Model could be used to explain a number of observed CR phenomena. Here, we are going to follow the SSM idea and go further up in energy to the very end of the cosmic ray energy spectrum.

Many of the experimentally observed features in the UHECR domain (*e.g.*, the anisotropy studies in [4]), confirm that we actually see there the vanishing Galactic component and the new Extra-Galactic (EG) one which starts to dominate above an energy of  $3 \times 10^{18}$  eV. The analysis of all available data made in [5] shows that the EG component may start as power-law with an index of about 2, and then, above about  $10^{19}$  eV, continue with observed index of  $\sim 3$  up to the end of measurements (*i.e.*,  $10^{20}$  eV or slightly higher).

The CR sources, especially for ultra high energies, are unknown. Two general classes of potential sources have been studied in the literature: (i) astrophysical objects, such as active galactic nuclei (AGN), quasars, and colliding galaxies (see, *e.g.*, [6]), where the usual cosmic matter constituents are accelerated to extremely high energies in so-called “bottom-up” processes; and (ii) some exotic “top-down” mechanisms such as the decay of (super-heavy) dark matter particles, topological defects, or monopoles (see, *e.g.*, [7]).

The serious problem for “bottom-up” theories is the UHECR general isotropy. There is no significant excess in any direction to a potential source.

In recent work, evidence has been presented that UHECR particles have a distribution of masses [8], generating obvious difficulties for “top-down” ideas. This finding is essential to the present work— a significant fraction of UHECR particles are multiply charged (up to  $Z = 26$  in the case of iron), which makes them more sensitive to extragalactic magnetic fields.

The “average” approach to UHECR spectrum calculations, found already in the first Greisen, Zatsepin, and Kuzmin [9, 10] papers, is to assume that because we know nothing about the sources, that for every point in space and time the production of UHECR is equally probable. The UHECR spectra shown in [10], but also the frequently quoted spectrum published by the AGASA group [11], were obtained assuming constant and uniformly distributed UHECR source power in the whole Universe. It gives a perfectly isotropic distribution of UHECR directions and a clear GZK cut off, which is the consequence of interactions of UHE nucleons with the 3 K cosmological microwave background photons. However, in the real Universe the distribution of matter is not exactly uniform. Structures known as galaxy clusters exist, and, if the UHECR sources are astrophysical, they should follow the usual matter (galaxies) distribution. Our Galaxy is within the Virgo cluster, about 15 Mpc from its center, and it is obvious that particles of energies above  $10^{19}$  eV, if created there, should point more or less exactly to their sources. Some

enhancement is actually seen, but it is statistically not very significant, and, as will be discussed in this paper, far too small when compared with expectations.

Assumptions about some particular, non-uniform distribution of UHECR sources in extragalactic space have also been carefully studied recently, in Refs. [12, 13]. The UHECR spectrum and small and large scale correlations (anisotropies) calculated there are significantly closer to the measured cosmic ray features than in models with a uniform source distribution.

The present work goes, in some senses, a step further in this direction. A single source is certainly far from isotropy, but here we also reject the assumption about its constancy in time. This introduces an additional parameter—the dimension of time, but at the expense of requiring an essentially new solution of the general anisotropy problem, as will be shown below.

For a continuous UHECR source, the very energetic particles should propagate along (nearly) straight lines, reaching the observer after a time  $\approx R/c$  and giving evident directional correlation with some astrophysical objects, which is not the case in practice.

We will discuss here the possibility that the UHECR sources are of transient nature—that they are in an active state for some time, say  $10^{7-9}$  years (an interval so big that it covers the collision time for galaxies passing each other, the estimated time of activity of AGN, etc.), and then remain quiet. UHECR are assumed to be produced only in the active phase. The idea is that the bulk of UHECR were produced by one or a few sources located relatively nearby (on the extragalactic scale), but which are at present not active. This is a simple solution of the isotropy problem. The very energetic particles traveling rectilinearly have passed Earth already, and what we see now as the UHECR flux is only those particles which are deviated enough by extragalactic magnetic fields to be delayed, relative to the light signal, by a substantial amount of time.

The only problem is to see if such a mechanism can really work—if the magnetic fields are strong enough to curve the trajectories of particles of energies around  $10^{20}$  eV.

## 2 Propagation of UHECR in the Intergalactic Magnetic Field

The UHECR under consideration are electrically charged, so their propagation in intergalactic space is therefore affected by the magnetic fields along their path. The intergalactic magnetic field strength is believed to be on the order of  $10^{-8}$ – $10^{-9}$  G, and for the distances of interest of about 1–100 Mpc and particle energies above  $10^{18}$  eV, some deviations from rectilinear propagation are expected.

Experimental knowledge of large-scale magnetic fields is rather scarce (see, for example, [14] and discussions given in [15] and [16]). These fields will have both regular and random components. The former can be, in principle, a relic of distant epochs (occasionally compressed and magnified or amplified by dynamo-like mechanisms). However, at present we have no evidence of the existence of such, so we neglect it.

The irregular component is present in intergalactic space, as it is in our Galaxy (and others). Its source can be ionized plasma emitted by galaxies and clusters of galaxies,

some of which will have come from supernova remnants bursting out of the host galaxies. The escape of galactic cosmic rays into the intergalactic medium (IGM) is a special case of this “process.” Insofar as the energy density of cosmic rays in the IGM—coming from escape from galaxies, is  $\sim 10^{-6} \text{ eV cm}^{-3}$  (obtained by integrating the extragalactic flux of cosmic rays), the corresponding magnetic energy density will give an rms field of  $\sim 3 \times 10^{-9} \text{ G}$  assuming equipartition. Another source of extragalactic magnetic field is from active galactic nuclei and other near-cataclysmic events. The magnetic disturbances evolve in time in accordance with the conventional turbulence picture, transferring energy consecutively down to smaller scales where the energy is finally dissipated.

There are various possibilities for the manner in which particles propagate through the IGM, but here we consider just two: the cubic domain model and the Kolmogorov turbulence model.

We now examine how the particular random field structure influences UHECR propagation across large distances.

## 2.1 Cubic domain model for the random magnetic field

The transport of charged particles when well-known conditions are fulfilled can be described as a diffusion process. The diffusion itself can be thought of as the limit of the constant step random walk process, this being defined by one parameter only: the length of a single step.

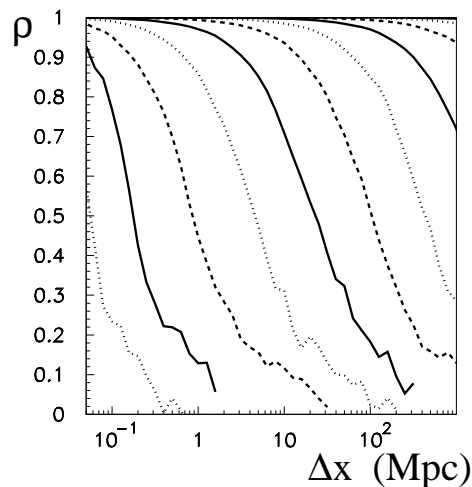


**Fig. 1** The velocity direction correlation coefficient for the cubic domain model of the random magnetic field shown as a function of separation distance for different proton energies. The solid lines represent energies of  $10^{18}$ ,  $10^{19}$ ,  $10^{20}$ , and  $10^{21} \text{ eV}$  (from the least correlated to the one close to 1 for almost all distances), dashed and dotted 2 and 5 times these values, respectively.

On the other hand, there is a limit to the large-scale random magnetic field arising from the results of Faraday rotation measurements. It can be said that

$$\langle \mathbf{B}_{\parallel} \rangle \times \sqrt{\lambda_B} < 10^{-9} \text{ G Mpc}^{1/2}, \quad (1)$$

where  $\lambda_B$  is the magnetic field coherence length, which can be treated as the distance over which the orientation of the magnetic field changes randomly. The simplest model of a chaotic magnetic field is just the cubic domain model, in which the space is divided into equal cubic cells of size  $\lambda_{\text{cell}}$ , the field in each cell is equal to  $\langle B \rangle$ , and its orientation changes randomly from cell to cell.

In such a picture, due to the fact that the cubic lattice orientation as a whole is obviously not fixed, the effective coherence length  $\lambda_B$  is defined precisely as

$$\int \mathbf{B}(\mathbf{x}) \cdot \mathbf{B}(\mathbf{0}) d\mathbf{l} = \langle \mathbf{B}^2 \rangle \lambda_B \quad (2)$$

(where the integration goes along the straight line over a distance much greater than any of the regular component scales of  $\mathbf{B}$ ).  $\lambda_B$  is not exactly equal to  $\lambda_{\text{cell}}$ , but the difference for our purposes (extragalactic UHECR propagation) is not significant.

The magnetic field coherence length in the case of UHECR cannot be used as a random walk step size for the propagation calculations. If the Larmor radius of a particle of charge  $Z$  and energy  $E$  is bigger than  $\lambda_B$ , then after traversing the distance  $\lambda_B$  the particle velocity still remembers (on average) its initial direction.

To find out the random walk step length, we performed simulations of charged particles in a magnetic cubic lattice of size 0.1 Mpc with a random magnetic field of 10 nG. This is comparable with the Larmor radius ( $\propto E/(ZB)$ ) for protons of energy  $10^{18}$  eV. The propagation coherence length  $\lambda_c$  is defined, by analogy with Eq.(2), as

$$\int \mathbf{v}(\mathbf{x}) \cdot \mathbf{v}(\mathbf{0}) d\mathbf{l} = \langle \mathbf{v}^2 \rangle \lambda_c. \quad (3)$$

The integration is similar to that in Eq.(2). It is a function of particle charge and energy.

To study this in more detail, we plot in Fig.1 the correlation coefficient for the proton velocity direction defined as

$$\rho(\Delta \mathbf{x}) = \frac{\langle \mathbf{v}(\mathbf{x}) \cdot \mathbf{v}(\mathbf{x} + \Delta \mathbf{x}) \rangle}{\langle \mathbf{v}^2 \rangle} \quad (4)$$

for different energies traversing our cubic magnetic domain space (where energy losses are neglected).

## 2.2 A turbulent random magnetic field

A more realistic picture of the intergalactic magnetic field uses the Fourier modes and their power spectrum

$$\mathbf{B}(\mathbf{x}) = \int \frac{d^3 \mathbf{k}}{(2\pi)^3} \mathbf{B}(\mathbf{k}) e^{i(\mathbf{k} \cdot \mathbf{x} + \phi(\mathbf{k}))}, \quad (5)$$

where  $\phi(\mathbf{k})$  are random phases, and  $2\pi/L_{\text{min}} < k < 2\pi/L_{\text{max}}$  with  $L_{\text{min}}$  and  $L_{\text{max}}$  are the lower and upper limits of the magnetic field turbulence scales, respectively.

In the present paper, a particular turbulent random field was realized by replacing the integration in Eq.(5) by the sum of 1000 independent Fourier components, each with

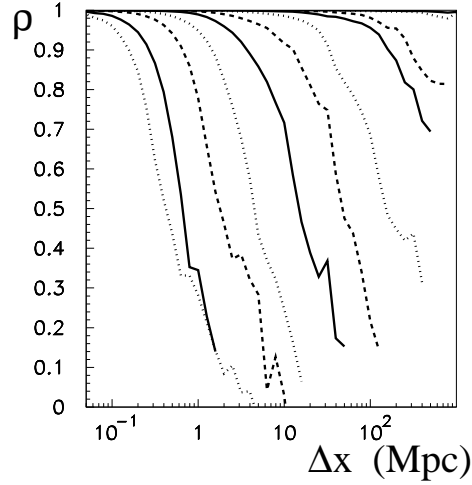


**Fig. 2** The velocity direction correlation coefficient for the Kolmogorov turbulent magnetic field model. The key to the lines is as given in Fig.1.

randomly chosen value of  $k$  (limited by  $L_{\min}$  and  $L_{\max}$ ) and random phase  $\phi$ . The sum was then normalized to yield the assumed  $\langle |\mathbf{B}(\mathbf{x})|^2 \rangle$ . In the calculations, we have used  $\langle |B| \rangle = 2 \times 10^{-9}$  G and  $L_{\min} = 0.01 \div 0.1$  Mpc and  $L_{\max} = 2$  Mpc. Concerning the UHECR transport problem, the lower turbulence size limit is of no importance, and the upper limit (in the reasonable range given above) has only a minor influence on the normalization of  $\langle |B| \rangle$ . The average value of  $\mathbf{B}^2$  here is different from the one assumed for the cubic cell model (as well as the scale of its irregularities), but the propagation of charged particles just for such values is similar in both models, as will be shown below.

The power spectrum  $B^2(k)$  is proportional to the energy density contained in the  $\mathbf{k}$  mode. For the power-law turbulence spectrum,

$$B^2(k) \sim \langle |\mathbf{B}(\mathbf{x})|^2 \rangle k^{-n}. \quad (6)$$

For the general case of Kolmogorov turbulence, the index  $n$  is equal to  $5/3$ . The magnetic field coherence length for this case can be calculated analytically [15] and is equal to  $L_{\max}/5$  for small  $L_{\min}/L_{\max}$ .

For proton propagation in the Kolmogorov turbulent magnetic field, the correlation coefficient for velocity direction  $\rho$  given by Eq.(4) has been calculated and the results are given in Fig.2.

### 2.3 Comparison of particle propagation in random magnetic field models

The propagation coherence length  $\lambda_c$  defined in Eq.(3) for the turbulent medium in comparison with the one for the cubic domain model is shown in Fig.3.

It can be seen from all the figures that the transport of charged particles in the two types of random magnetic field model should be very similar, in spite of the fact that the detailed structure of the field is so very different. Not only is the average magnetic field

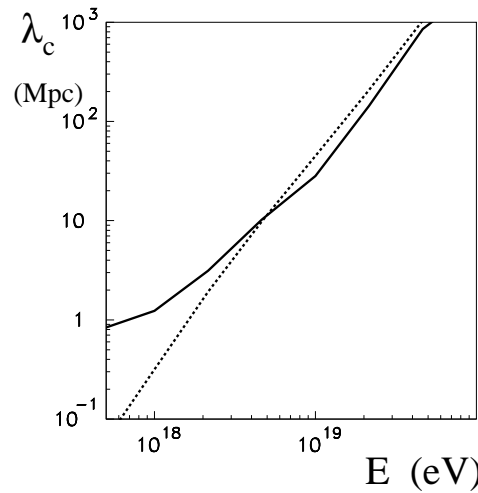


**Fig. 3** The propagation coherence length for the Kolmogorov turbulent magnetic field model (solid line) and the cubic domain model (dashed line), for which  $\lambda_c \propto E^2$ .

strength  $\langle |B| \rangle$  different ( $10 \times 10^{-9}$  G for cubic domains and  $2 \times 10^{-9}$  G for a Kolmogorov turbulent medium), but the spectrum of the field is different. The spectrum  $\langle B^2(k) \rangle$  calculated by Fourier decomposition of generated chaotic fields in each model, and the respective magnetic field correlation coefficients, are shown in Figs. 4 and 5.

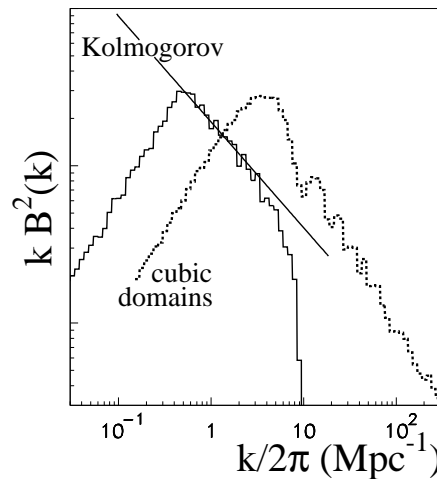


**Fig. 4** The powers of Fourier components calculated for the Kolmogorov turbulent magnetic field model ( $L_{\min}$  and  $L_{\max}$  are 0.1 and 2 Mpc) and the cubic domain model (with a cell size equal to 0.1 Mpc); the straight line represents  $k^{-5/3+1}$  dependence. At right, the magnetic field correlation coefficient for each model.

For a given energy, if the observer is located at a distance bigger than  $\lambda_c$ , as shown in Fig.3, the propagation is diffusive. The deviation from rectilinear propagation starts around  $\lambda_c$ . This can be seen in Figs. 6 and 7, where the mean distance reached by the particle as a function of time is shown, and where the distance distributions are given. For rectilinear propagation, the respective line slope is approximately unity (on a log×log) plot; when the diffusion starts to dominate, the slope changes from 1 to 1/2. It



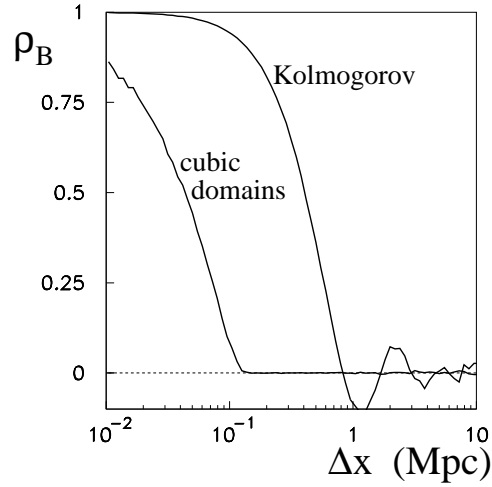


**Fig. 5** The magnetic field correlation coefficients for the Kolmogorov turbulent magnetic field model and the cubic domain model. (parameters as in Fig.4).

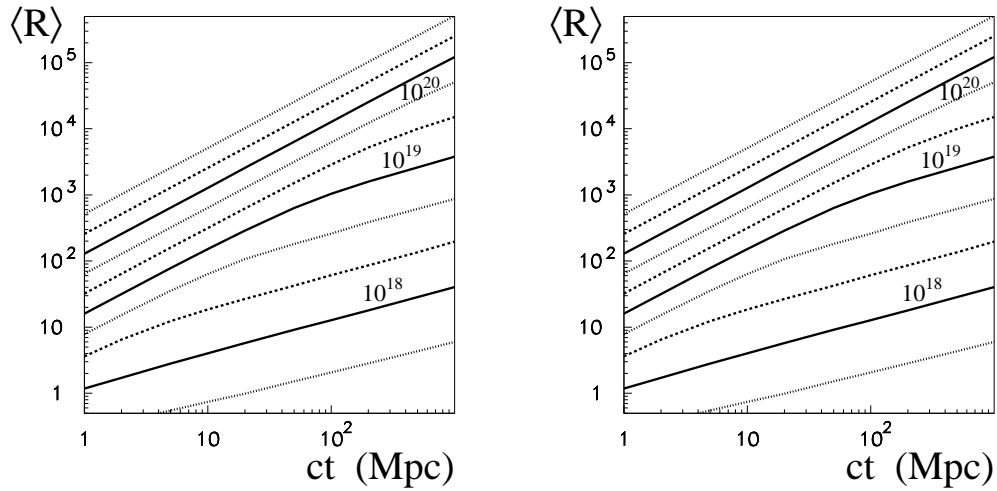


**Fig. 6** Mean distance traveled by protons during time  $t$  for the Kolmogorov turbulent magnetic field model (left) and for the cubic domain model (right). A vertical shift was introduced to separate the lines for each particle energy. Parameters:  $L_{\min} = 0.1$  Mpc and  $L_{\max} = 2$  Mpc;  $\langle B^2 \rangle = 2 \times 10^{-9}$  G for the Kolmogorov turbulent medium, and  $\langle B^2 \rangle = 10^{-8}$  G and  $\lambda_{\text{cell}} = 0.1$  Mpc for the cubic domain model.

is seen that particles with energies of  $10^{18}$  eV diffuse while those with energies of  $10^{20}$  eV propagate along (almost) straight lines, through distances of the order of Gpc.

### 3 Energy loss processes

The UHECR domain is quite rich in physical processes involving energy losses. Starting with protons of relatively low energies, about  $10^{18}$  eV,  $e^+e^-$  pair production on the cosmic microwave background (CMB) photons starts to play a role, which reaches maximal importance slightly below  $10^{19}$  eV. The main GZK process of energy loss is due to  $\Delta$



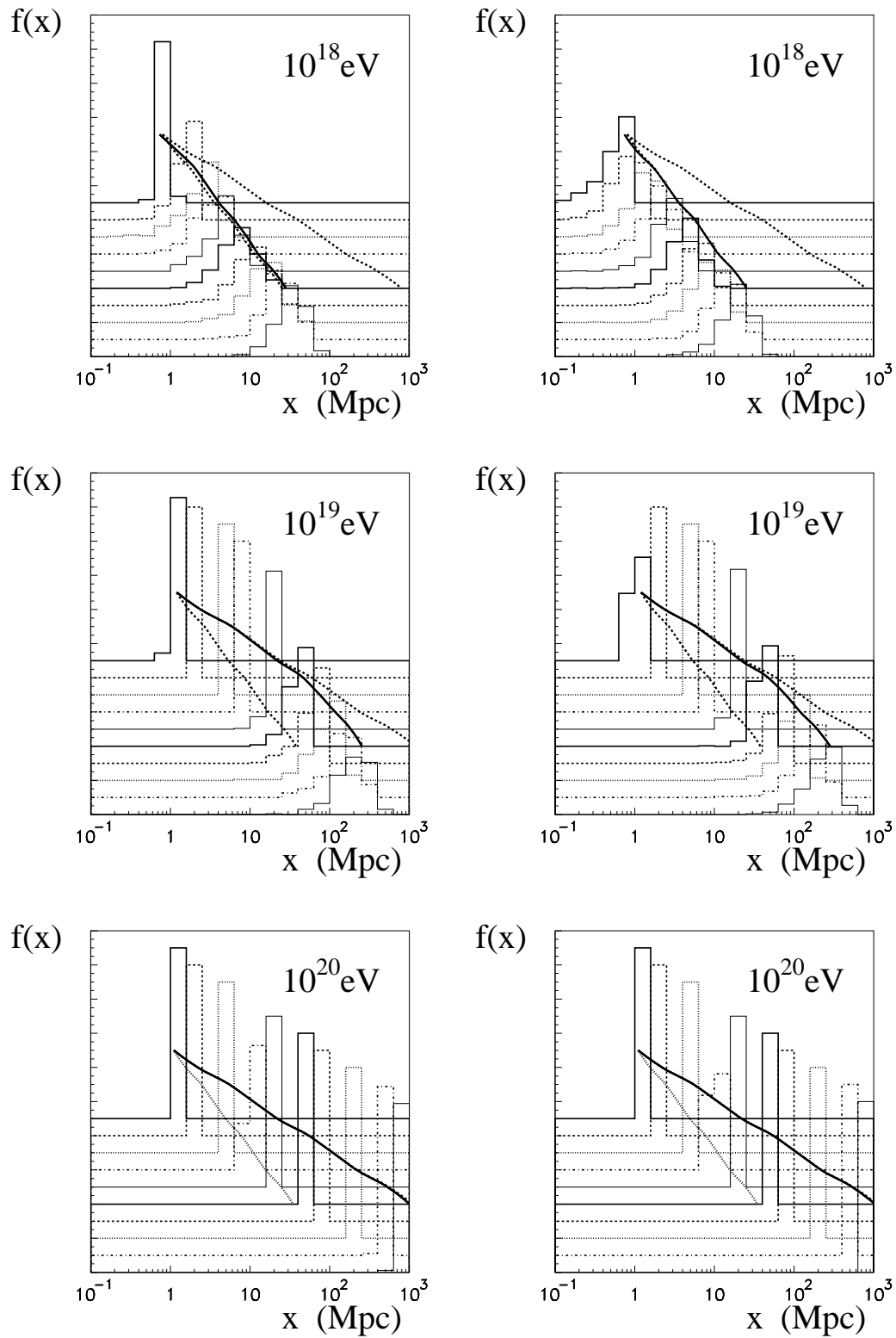


**Fig. 7** Distributions of distance from source at different times of propagation  $ct = 1, 2, 5, 10, 20, 50, 100, 200, 500$ , and  $1000$  Mpc (from top to bottom—the distributions are shifted vertically). Inclined lines show the positions of the average values: dashed for the rectilinear propagation ( $R = ct$ ), dotted for diffusion ( $R \sim \sqrt{t}$ ), and solid for the actual average as in Fig. 6. The figures to the left are for the cubic domain model, and those to the right for the Kolmogorov turbulent random magnetic field.

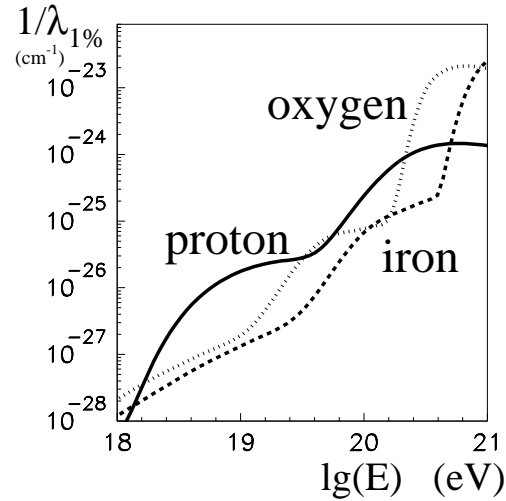


**Fig. 8** Inverse mean length for 1% energy loss for iron, nitrogen, and protons on extragalactic background photons.

resonance excitation (and its subsequent decay, dissipating energy, eventually to low energy  $\gamma$ s) on CMB photons. The energy losses of heavier nuclei relative to electron-positron pair creation are  $Z^2$  stronger, but, due to the different rest mass and therefore different Lorentz factor, the respective total nucleus energy should be  $A$  times higher than that for protons. The same scaling in energy ought to be applied for  $\Delta$  resonance creation (but without the  $Z^2$  enhancement). This makes the GZK mechanism for heavy nuclei not as important. The dominating process for nuclei is photo-disintegration on background photons. The significant rise in fragmentation cross section just at the energies of our present interest is due to the existence of giant dipole resonance. This excitation energy is close to 20 MeV for (almost) all interesting heavy nuclei. This is about one order of magnitude below the  $\Delta$  resonance excitation energy, and thus, if only the collisions with CMB photons are considered, the threshold energy for nuclear disintegration is of order  $A/10$  higher than the proton GZK cut-off energy. A review of the whole situation is presented in Fig.8 .

To compare the  $e^+e^-$  pair production,  $\Delta$  resonance creation by nucleons, and disintegration of heavy nuclei, the cross sections have to be convoluted, not only with the photon energy spectrum, but also with the inelasticity of the respective process. In Fig.8, the inverse average length for 1% energy loss is shown. It is different from the commonly used  $(d \ln(E)/dx)^{-1}$  describing the average length for losing a  $(1 - e^{-1} \approx 63\%)$  fraction of particle energy. But it is actually more illustrative specifically for cases where cross sections change substantially with the energy (by more than a decade for nuclei above  $10^{20}$  eV when the energy changes by  $e^{-1}$ ). Anyway, the difference between our  $\lambda_{1\%}$  and  $(d \ln(E)/dx)^{-1}$  is in the constant factor  $\approx 0.63/0.01$  by which the vertical scale in Fig.8 should be multiplied to match the convention.

The CMB is assumed to be of temperature 2.7 K and for higher energy photons we take the spectrum obtained in [17](the one labeled there the “best estimate” intergalactic

IRB).

Simulations of particle transport in both magnetic field models described above were performed assuming that their source emits protons and composite nuclei each time in newly generated field realizations. The particle trajectory was calculated in small steps of 3 kpc (3 kpc/ $c$  in time intervals). In each step, the field was assumed constant and the trajectory was calculated analytically, giving position and velocity direction for the traced particle after certain short time intervals.

Continuous energy losses were taken into account by diminishing the particle energy after each step. Abrupt losses of particle energy due to photo-pion production and spallation in the case of nuclei were included by generating in each step the actual interaction lengths for reactions with one or two nucleons released (n, p, 2n, pn, 2p separately) according to cross sections given in Ref.[19]. If the shortest of these interaction lengths was within the spatial step length, the length of the step was reduced to this value and the actual position of the interaction point (and particle direction there) was calculated. In the case of photo-pion reaction, the average energy loss due to  $\Delta$  resonance decay was subtracted. For nuclei, all the secondary products were included in the memory, to be propagated along with the initial nuclei until they were eventually lost after reaching the overall energy threshold, or until the propagation time limit (3 Gpc/ $c$  for the present calculations) was reached.

During propagation, particles were recorded each time they were within a spherical shell of thickness of 100 kpc and radius 3, 5, 7, 10, 15,... Mpc around the source. Their direction, energy, type (mass number), and time since emission (or since the emission of their initial progenitor) were later used to obtain the distributions of interest.

The initial energy spectrum was sampled in very short intervals in logarithmic scale and integrated, weighting events by the power-law emission spectrum (with a differential index of 2.1 for this paper).

## 4 Small scale clustering of UHECR

The UHECR, if they come from a relatively close source, are expected to be directionally correlated. Their arrival directions could point to the particular source in the sky. Several attempts have been made to verify this hypothesis, but all are based on limited statistics, and their significance has been limited.

We present here some results concerning the existence of small scale clusters relevant to the subject of the present paper. Our analysis is similar to the one in [18] based on the whole available Northern hemisphere data on cosmic ray events of energies above  $4 \times 10^{19}$  eV. The data consist of 113 events from AGASA, Haverah Park, Yakutsk, and Volcano Ranch experiments (19 of them with energies greater than  $10^{20}$  eV). We used a technique which was developed in searches for correlations among particles created in high energy accelerator experiments. Factorial moments in integral form are the best tools to be used for our purpose. Precisely, we used the so-called “star integral” method

for factorial moment calculations discussed extensively in [20] and defined as

$$F_k(\Delta) = \frac{\int \rho_k(y_1, y_2, \dots, y_k) \Theta_{12} \Theta_{13} \dots \Theta_{1k} dy_1 dy_2 \dots dy_k}{\int \rho_1(y_1) \rho_1(y_2) \dots \rho_1(y_k) \Theta_{12} \Theta_{13} \dots \Theta_{1k} dy_1 dy_2 \dots dy_k}, \quad (7)$$

where  $\rho_k(y_1, y_2, \dots, y_k)$  is the  $k$ -dimensional probability density, and  $\Theta_{ij}$  are equal to Heaviside step functions with argument  $(\Delta - \|y_i, y_j\|)$ :

$$\Theta_{ij} = \begin{cases} 1 & \text{if } \|y_i, y_j\| \leq \Delta \\ 0 & \text{if } \|y_i, y_j\| > \Delta \end{cases} \quad (8)$$

where  $\|y_i, y_j\|$  is the distance between two points defined in our case as the angle between directions of UHECR events. The interpretation of factorial moments in integral form, thanks to the  $\Theta_{ij}$  functions, is clear. The factorial moment gives the number of groups of events (doublets, triplets etc.) where the relative distances within each group are smaller than  $\Delta$  in the data sample analyzed, normalized by the number of such groups calculated for the sample with the same marginal distribution for all  $y_i$  variables and lack of any correlation among any of them, *i.e.*, where  $\rho_{k \text{ norm}}(y_1, y_2, \dots, y_k) = \rho_1(y_1) \rho_1(y_2) \dots \rho_1(y_k)$ .

The normalization factor can be obtained using the “event mixing” method, but in general, factorial moments can be used for comparison of observations with any model for the background.

Due to the small statistics, only the first two orders could be studied with some confidence. The factorial moments are related to integral cumulant moments  $K$ :

$$K_2 = F_2 - 1, \quad K_3 = F_3 - 3 F_2 + 2 \quad (9)$$

which represent genuine correlation of the given order present in the sample analyzed.

In Fig. 9, results concerning two-point correlations are shown. The observations are represented in the figures as the thick solid histogram. To see the significance of the observed correlation, upper limits can be calculated exactly using the Monte Carlo method by generating hundreds of thousands of times the uncorrelated “mixed events” pools and counting fractions of events exceeding each value of  $\delta$ . The limits are shown as dotted histograms for confidence levels of 90%, 95%, 99%, and 99.9%.

The analysis has been performed for two event samples. In the first data sample (labeled as “low E” in the figures), all events with energy of more than  $4 \times 10^{19}$  eV were used and for the second (“high E”), it was required that at least one event in the doublet or triplet had to be of energy greater than  $10^{20}$  eV. Such a division gives the possibility of checking if the correlation is indeed increasing with the particle energy, as one would expect.

Results on third order factorial moments and cumulants are shown in Fig. 10.

Concerning doublets analysis ( $F_2$ ), clustering appearing below  $3\text{--}4^\circ$  can be seen for both data samples. The probability that this is pure coincidence is of the order of 1%. For triplets ( $F_3$ ), the same can be said, suggesting that very close events may really exist in the data (but they are still at low confidence level).

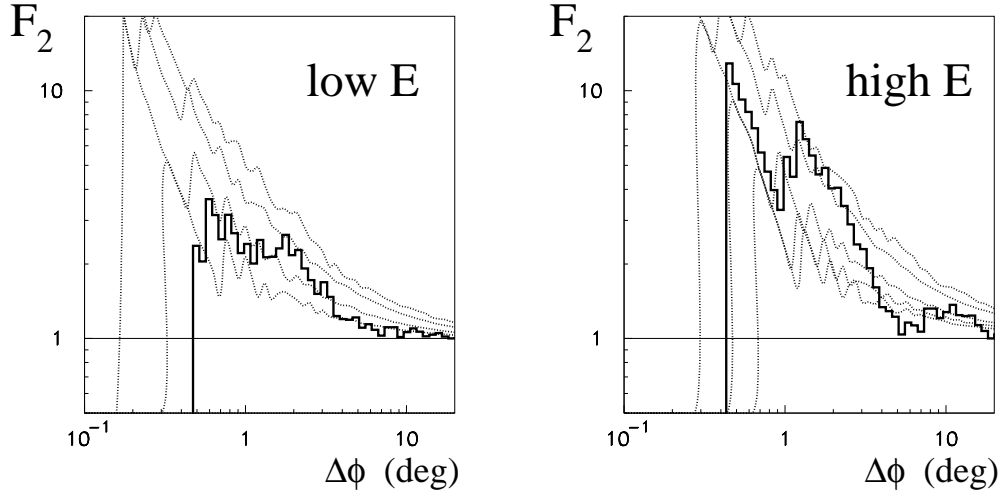


**Fig. 9** Second factorial moment calculated for all event sample (“low E”—left), and for pairs for which at last one event in the pair is of energy greater than  $10^{20}$  eV (“high E”—right). The result of the data analysis is shown by the solid histogram. Dotted lines represent the 90%, 95%, 99%, and 99.9% confidence limits, respectively.

It is known [18] that there is one very close triplet in the data. Its angular dimension is of the order of experimental angle determination accuracy, estimated to be a few degrees. There is a possibility that it is a real cluster correlated with a UHECR source superimposed on all the other isotropic UHECR directions. To generalize this concept (however the low (1-5) percent confidence is too small for any radical claims), we can try to find out how strong the real correlation should be to produce the effect. The hypothesis in question is that UHECR arrive in most cases from completely random directions, but there is a small probability that the single UHECR event is accompanied by another one from the same (within a few degrees) direction. The factorial moment method allows us to examine this hypothesis in a straightforward way. Making the “mixing event sample” to evaluate the denominator in Eq.(8), we can make it in a not exactly random way, but in the way described above, introducing a new parameter—the probability of accompaniment. With such a constructed reference sample, the full analysis can be performed, giving as a result the cumulants equal to 0 (and  $F_2$  equal to 1), if the real data follow the “additional accompaniment” idea.

In Fig. 11, we present the results of such an analysis with the additional accompaniment probability equal to 3%. This means that on average, the “mixed sample” contains a few ( $\sim 3$ ) close artificial doublets (there are 113 events in the sample) for the “low energy” case (all events with  $E > 4 \times 10^{19}$  eV). This is certainly not a big number, but one can see that the difference it makes is quite substantial. Summarizing, the existence of close clusters of UHECR, if real (hypothesis verified by existing data at the 95-99% confidence level), can be interpreted as the small, on the level of one percent, probability that there exist a few UHECR sources emitting particles reaching Earth with directions pointing to the source. Because we are working with statistics of correlated events in the data of order of a few, there is nothing more which can be said with reasonable confidence.

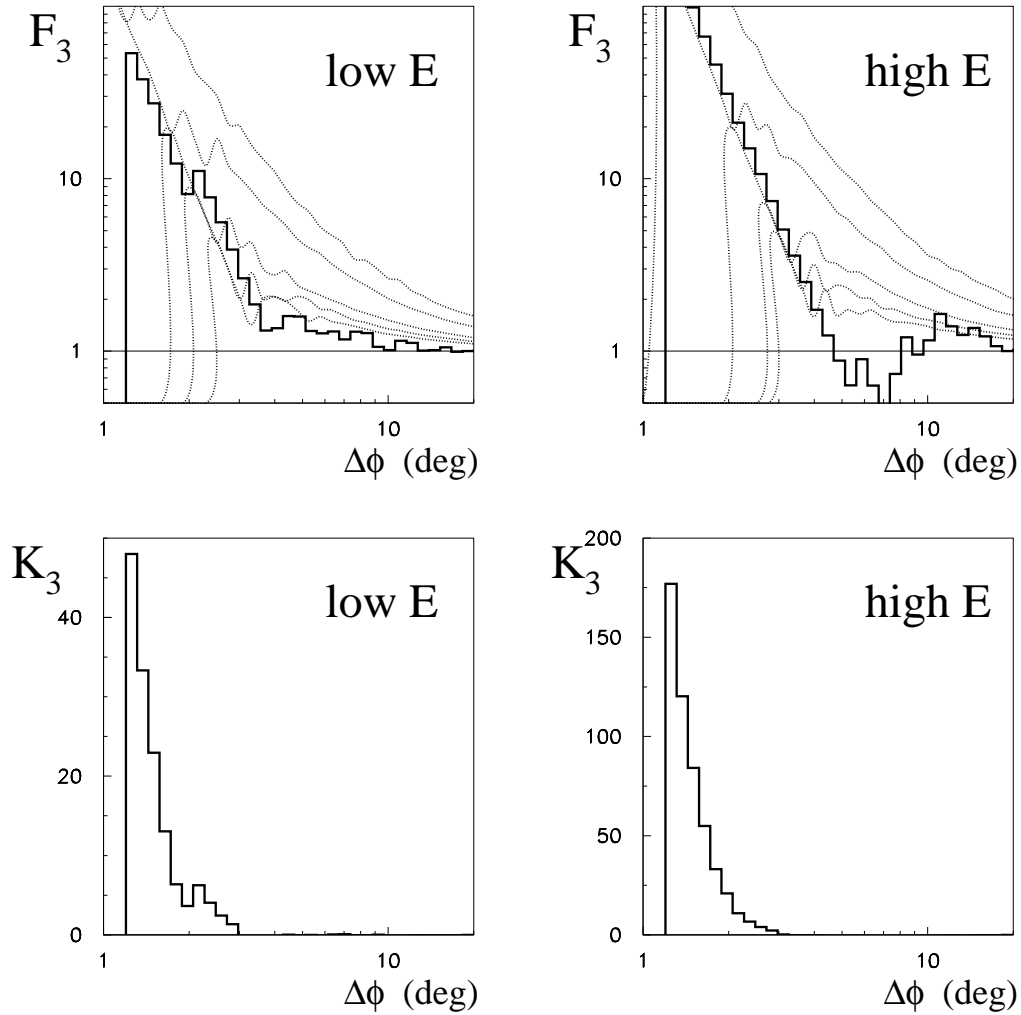


**Fig. 10** Third order factorial moments (top) and cumulants (bottom) showing genuine threefold correlation calculated for all event sample (left) and the one representing higher energy event triplets (right).

## 5 Deviation angles

### 5.1 Non-interacting protons

To examine the small scale clustering (at most on the few percent level, as was shown above), and to answer the questions: (i) do they create a nuisance for the “single UHECR source” model, and, (ii) in general, what are predictions for the propagation calculations in realistic intergalactic magnetic fields, and what deviations can be expected, extensive Monte Carlo calculations are needed.

For a given particle energy, the angle between the direction to the source and the observed particle velocity is called the deviation angle. This angle depends finally on the distance from the source and the time of particle propagation. Even for particle energies and distances for which rectilinear propagation dominates, there are particle trajectory fluctuations which allow the particle to be observed long after the  $R/c$  time and with big

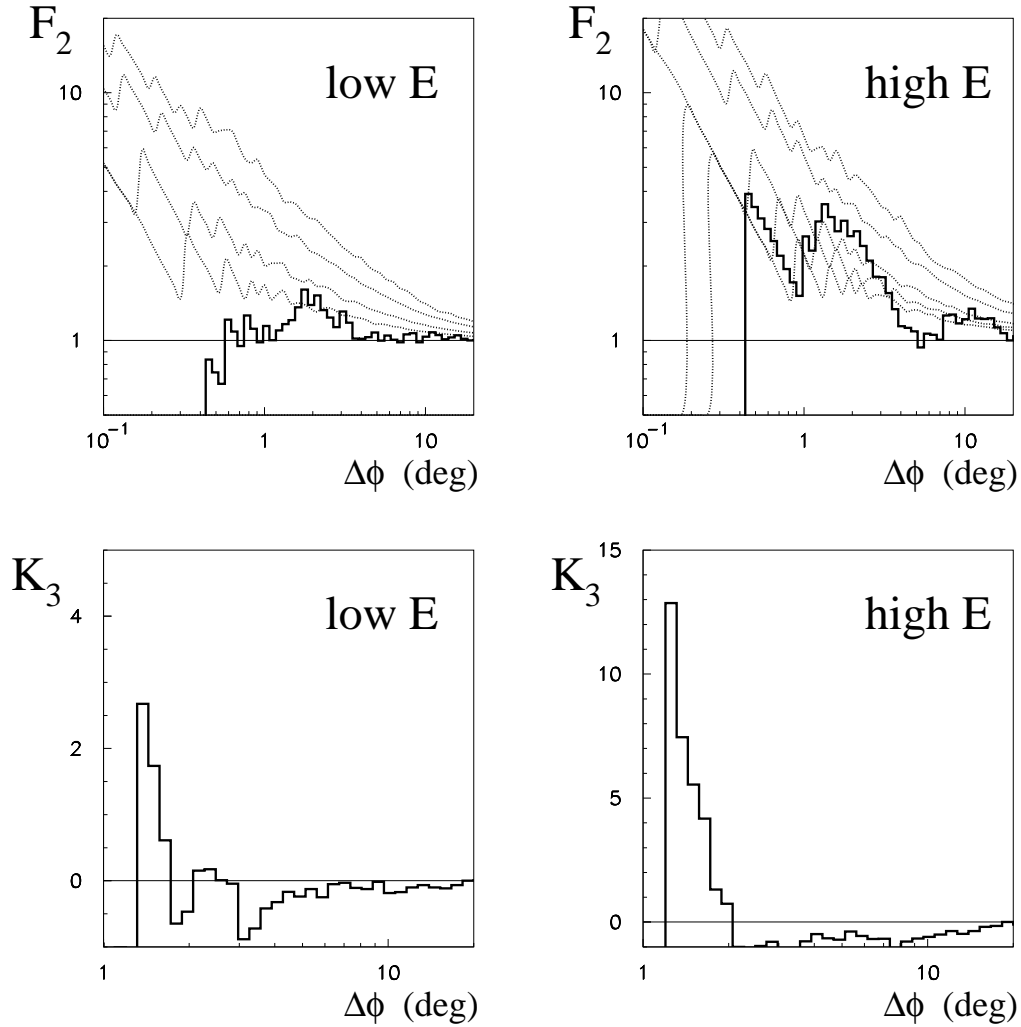


**Fig. 11** Second order factorial moments and third order cumulants for the model with artificially introduced correlation (accompaniment probability of 3%) calculated for all triplets (“low E”) and only for those including one UHECR of energy greater than  $10^{20}$  eV (“high E”).

deviation angles. Because we are interested in fractions of events as small as 3%, these fluctuations could be important.

To see the effects of the extragalactic magnetic field, the calculations were first performed for singly charged particles without any energy loss processes. In Table 1, the fractions of particles arriving in given delay time intervals are given, and in Table 2, average deviation angles are given for different particle energies and source distances with five ranges of delay time (with respect to the light signal). The first delay time range contains UHECR which propagate almost rectilinearly, and the last range contains the diffusive component whose velocities are oriented completely randomly.

It can be easily seen that for singly charged particles of energies of about  $5 \times 10^{19}$  eV, if the source is within  $\approx 15$  Mpc, the propagation is almost rectilinear, delay times are not bigger than  $10^6$  years, and mean deviation angles are less than  $10^\circ$ . For particles of energy greater than  $10^{20}$  eV, the mean deviation is very small, even if the particles come



5 Mpc	$5 \times 10^{17}$	$10^{18}$	$2 \times$	$5 \times$	$10^{19}$	$2 \times$	$5 \times$	$10^{20}$	$2 \times$	$5 \times$	$10^{21}$
$\tau < 10^5$				2	18	86	100	100	100	100	100
$10^5 < \tau < 10^6$			1	22	70	12					
$10^6 < \tau < 10^7$		1	10	29	4						
$10^7 < \tau < 10^8$	2	6	24	13							
$\tau > 10^8$	98	93	65	34	8	2					

15 Mpc	$5 \times 10^{17}$	$10^{18}$	$2 \times$	$5 \times$	$10^{19}$	$2 \times$	$5 \times$	$10^{20}$	$2 \times$	$5 \times$	$10^{21}$
$\tau < 10^5$						2	42	91	100	100	100
$10^5 < \tau < 10^6$					4	72	57	9			
$10^6 < \tau < 10^7$				6	34	22	1				
$10^7 < \tau < 10^8$			2	17	15						
$\tau > 10^8$	100	100	98	77	47	4					

50 Mpc	$5 \times 10^{17}$	$10^{18}$	$2 \times$	$5 \times$	$10^{19}$	$2 \times$	$5 \times$	$10^{20}$	$2 \times$	$5 \times$	$10^{21}$
$\tau < 10^5$								4	60	94	100
$10^5 < \tau < 10^6$							23	78	37	6	
$10^6 < \tau < 10^7$						27	65	18	2		
$10^7 < \tau < 10^8$					6	22	7				
$\tau > 10^8$	100	100	100	100	94	51	6				

**Table 1** Fractions of cosmic ray flux (non-interacting protons) arriving in given delay time intervals for different particle energies at different distances to the source.

from 50 Mpc away.

The propagation of non-interacting particles scales with  $Z$ . To see what the situation is with iron nuclei, one has to look in Tables 1 and 2 for energies 26 times smaller. The iron nucleus of energy  $5 \times 10^{19}$  eV travels on average longer than  $10^8$  years and arrives almost isotropically even for sources as close as 5 Mpc. For a source at 15 Mpc and energy of  $10^{20}$  eV, still no trace of anisotropy can be expected.

This situation, however, can change if energy loss processes are taken into account. Particles traversing intergalactic space can interact with the matter and fields there. The longer they propagate, the bigger the energy losses are. It is expected that the general effect of UHECR interactions will be to favor the shorter paths, corresponding to smaller delays and deviation angles.

5 Mpc	$5 \times 10^{17}$	$10^{18}$	$2 \times$	$5 \times$	$10^{19}$	$2 \times$	$5 \times$	$10^{20}$	$2 \times$	$5 \times$	$10^{21}$
$\tau < 10^5$				9	6	5	3	1	1	<1	<1
$10^5 < \tau < 10^6$			27	21	17	12					
$10^6 < \tau < 10^7$		52	55	47	30						
$10^7 < \tau < 10^8$	79	77	78	81							
$\tau > 10^8$	90	90	90	90	90	90					

15 Mpc	$5 \times 10^{17}$	$10^{18}$	$2 \times$	$5 \times$	$10^{19}$	$2 \times$	$5 \times$	$10^{20}$	$2 \times$	$5 \times$	$10^{21}$
$\tau < 10^5$						6	4	3	1	1	<1
$10^5 < \tau < 10^6$					12	11	8	8			
$10^6 < \tau < 10^7$				37	30	23	25				
$10^7 < \tau < 10^8$			68	69	73						
$\tau > 10^8$	89	90	90	90	90	90					

50 Mpc	$5 \times 10^{17}$	$10^{18}$	$2 \times$	$5 \times$	$10^{19}$	$2 \times$	$5 \times$	$10^{20}$	$2 \times$	$5 \times$	$10^{21}$
$\tau < 10^5$								2	2	1	1
$10^5 < \tau < 10^6$							7	5	4	3	
$10^6 < \tau < 10^7$						20	15	13	10		
$10^7 < \tau < 10^8$					38	40	40				
$\tau > 10^8$	89	90	90	90	90	90	90				

**Table 2** Mean deviation angle for non-interacting protons propagating from a source located at different distances as a function of particle energy and delay time. For some particular values, the flux of particles is negligible, so the values cannot be given.

## 5.2 Introduction of energy loss processes

Results of calculations for the propagation of protons and iron nuclei are shown in Tables 3 and 4.

From Tables 3 and 4, for about 10% of the events, the mean deviation for iron nuclei is about  $40^\circ$  at an energy of  $5 \times 10^{19}$  eV. Going a little further up in particle energy, to  $10^{20}$  eV, approximately 20% have mean deviation angle of about  $20^\circ$  (delays less than  $10^7$  years) and the next 50% have mean deviation  $40^\circ$  and arrive not later than  $10^8$  years after the light signal. This is enough to see some slight enhancement of UHECR from the region on the sky where the source is (where galaxies collide? [6]), but obviously the general anisotropy constraint is still fulfilled. It is easy to achieve more or less anisotropy because there is some freedom with the magnetic fields (they can be eventually smaller

protons	$5 \times 10^{17}$	$10^{18}$	$2 \times$	$5 \times$	$10^{19}$	$2 \times$	$5 \times$	$10^{20}$	$2 \times$	$5 \times$	$10^{21}$
$\tau < 10^5$						2	29	98	100	100	100
$10^5 < \tau < 10^6$					2	71	71	2			
$10^6 < \tau < 10^7$				3	79	27					
$10^7 < \tau < 10^8$				25	10						
$\tau > 10^8$	100	100	100	72	9						

iron	$5 \times 10^{17}$	$10^{18}$	$2 \times$	$5 \times$	$10^{19}$	$2 \times$	$5 \times$	$10^{20}$	$2 \times$	$5 \times$	$10^{21}$
$\tau < 10^5$											
$10^5 < \tau < 10^6$									20		
$10^6 < \tau < 10^7$							1	18	61		
$10^7 < \tau < 10^8$							11	49	19		
$\tau > 10^8$	100	100	100	100	100	100	88	33			

**Table 3** Fractions of cosmic ray UHECR flux arriving in given delay time intervals for different (observed) (observed) energies. Source distance is 15 Mpc.

or larger than assumed in this work).

In the case of protons, however, if one wants to see them above  $10^{19}$  eV, a strong anisotropy has to be observed and the source must be active at present, so there is the general possibility of the identification of the UHECR source with some astrophysical object on the sky.

Concerning the small scale clustering problem, we have to say that between our results and the widely discussed in the literature existence vs. lack of coincidences between UHECR direction and astrophysical objects, two solutions are possible. The first is that the clustering is by pure chance coincidence, which can be accepted at the 95 or 99% confidence level. The second possibility is that there is only one relatively close source of UHECR active “at present” (or at least only a few sources) and protons from there form the cluster(s) in question. In this case, however, the bulk of UHECR events are produced in other sources, or in one “single source” which is “at present” not active.

A review of the actual experimental situation was presented in the XXVIII<sup>th</sup> International Cosmic Ray Conference in Tsukuba [21]. Recently, the AGASA group confirmed their findings of close doublets and triplets for energies from  $10^{19}$  eV to the very end of the spectrum, and the HiRes experiment does not see anything like this above  $10^{19}$  eV. The problem with high statistic monocular HiRes data is that the angular resolution is rather poor (and obviously not symmetrical). With such conditions, however, they give an upper limit for doublets and it is equal to 4. The more precise HiRes stereo data set consists only of 164 events above  $10^{19}$  eV, and nothing more significant than  $1\sigma$  is seen

protons	$5 \times 10^{17}$	$10^{18}$	$2 \times$	$5 \times$	$10^{19}$	$2 \times$	$5 \times$	$10^{20}$	$2 \times$	$5 \times$	$10^{21}$
$\tau < 10^5$					2	2	4	3	1	1	$<1$
$10^5 < \tau < 10^6$				4	12	11	7	5			
$10^6 < \tau < 10^7$			20	39	28	18	20				
$10^7 < \tau < 10^8$			62	57	59						
$\tau > 10^8$	90	90	90	90	90						

iron	$5 \times 10^{17}$	$10^{18}$	$2 \times$	$5 \times$	$10^{19}$	$2 \times$	$5 \times$	$10^{20}$	$2 \times$	$5 \times$	$10^{21}$
$\tau < 10^5$											
$10^5 < \tau < 10^6$				2	9	3	6	3	2		
$10^6 < \tau < 10^7$		58	19	20	15		24	24	29		
$10^7 < \tau < 10^8$		41	39	49		33	43	62	69		
$\tau > 10^8$	90	90	90	90	90	90	90	90			

**Table 4** Mean deviation angle for UHECR from the source located at 15 Mpc as a function of particle energy and delay time.

there. Both HiRes statements, in spite of being negative, do not contradict at a high significance level the AGASA statement. On the other hand (as was shown above), the significance of AGASA clustering is in fact only on the 95-99% confidence level.

## 6 Predicted UHECR flux

The exact propagation calculations were performed for different times of source activity. The source composition of protons and iron and oxygen nuclei was assumed, and their relative proportions were adjusted to the data on the extragalactic UHECR flux [5]. The continuous background consisting of cosmic rays produced by sources identical to the Single Source, uniformly distributed in the Universe (one per 1000 Mpc<sup>3</sup> per 10<sup>9</sup> years) was also assumed. Its contribution is given in Fig. 12 by the thin solid line. This background is about 10% of the total UHECR flux and does not play a significant role here.

The experimental points used in the present work are taken from the analysis of the Northern hemisphere “world data” given in Ref.[5]. The points shown in Fig.12 represent the combined UHECR spectrum from Haverah Park, AGASA, Volcano Ranch, Yakutsk and Fly’s Eye experiments, after subtraction of the galactic component (dominating still at about 10<sup>18</sup> eV, but negligible above 10<sup>19</sup> eV). The agreement between different measured data sets was achieved by adjusting the individual energy estimation accuracy and overall normalization. It was found satisfactory, thus allowing the authors to give

the extragalactic UHECR energy spectrum free of particular instrumental biases.

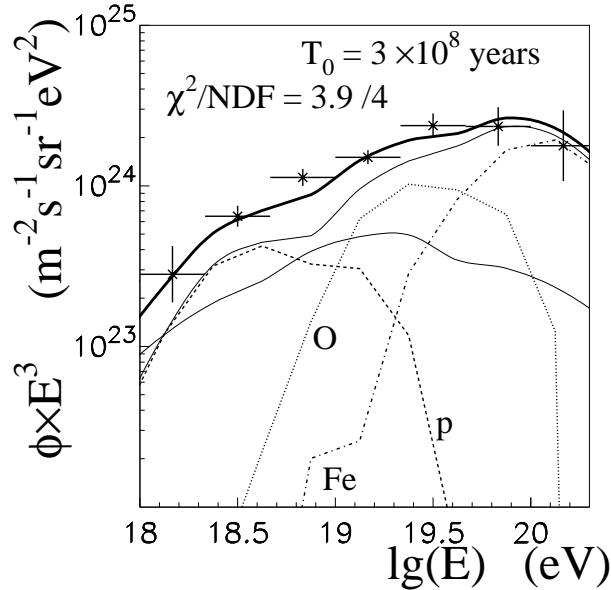


**Fig. 12** UHECR flux for Single Source. Source is located at 15 Mpc and switched off at the time  $T_0 = 3 \times 10^8$  years ago. The proton contribution is shown by dashed, iron by dot-dashed, and oxygen by dotted line. The source spectrum index is  $-2.1$ . The continuous background is shown by the thin solid line and was obtained assuming one random source per each  $1000 \text{ Mpc}^3 \times 10^9$  years.

The very recent discussion of the UHECR spectrum [22] and the discrepancies between the last reported AGASA spectrum which contains 11 events of energies above  $10^{20}$  eV and HiRes (mono and stereo) spectra (compatible with the Fly’s Eye spectrum) with only 2 such cases with comparable exposures shows that there is, probably, systematic bias in energy determination on the order of 30% in one of the experiments. The method of combining energy spectra applied in Ref.[5] takes into account such uncertainties. Thus, experimental points in Fig.12 represent well the actual situation in the UHE region. The problem of whether the GZK cut-off exists (as claimed by the AGASA group) or not (according to HiRes) is still an open question, but the data seems to be as shown in the figure.

The number of parameters adjusted to the seven points representing extragalactic UHECR flux at first sight seems to be unreasonably big: normalization, composition (2 parameters), source spectral index,  $T_0$ , source activity duration time, distance to the source, background normalization (density of the sources averaged in large space and time intervals)— all together eight of them. This is big if all of the parameters are uncorrelated. But they are in fact strongly correlated, and the freedom of choice does not represent the real number of degrees of freedom of the fitting procedure.

It is clear that the “best” spectrum shown in Fig.12 does not match exactly the experimental points used. Additionally, it can be mentioned here that some of these parameters are fixed to some reasonable boundaries (as spectral index or background normalization). In general the main purpose of the present paper is not to fit the data

perfectly by a single line; the uncertainties of many astrophysical parameters of extragalactic space (magnetic field structure, matter and radiation densities, etc.) and the limited statistics of registered UHECR events do not permit the derivation of any strong physical conclusions from this kind of fit. We want, rather, to show only that general agreement (or, more precisely, lack of experimental contradiction) can be achieved within the proposed UHECR origin model. Thus the particular values of  $T_0$ , p:O:Fe composition, and distance to the source taken to draw the lines in Fig.12 should be treated not as the main result of this work, but rather as an example, showing that with values like these, quite satisfactory agreement between the “single UHECR source model” and the measured extragalactic UHECR spectrum can be obtained.

Our fit to the UHECR spectrum was found with the Single Source inactive for the last  $3 \times 10^8$  years. The composition (p:O:Fe about 10:5:3) is not extraordinary if compared with the one derived from experimental information in the energy region of about three orders of magnitude lower, *i.e.*, at “the knee.” It is important to mention that for such “light” source composition, the observed UHECR flux above  $3 \times 10^{19}$  eV is quite heavy, and above  $10^{20}$  eV is completely iron-dominated.

More detailed discussion of the particular parameter values obtained is given in [16].

## 7 Conclusions

Extensive Monte Carlo calculations for the propagation of UHECR in extragalactic magnetic fields have been performed.

The directional small scale clustering in the available data gives a 5% limit on its chance origin. The data are consistent with the hypothesis that the overall isotropic UHECR direction distribution is enhanced by the additional clustering probability on the level of no more than a few ( $\sim 3$ ) percent of observed UHECR events. Propagation calculations show that such enhancement can be related to primary protons from only the source (or sources) active at present.

It is possible that the bulk of the UHECR are created in a Single Source at 15 Mpc distance which was active about  $3 \times 10^8$  years ago. This model is consistent with the large scale anisotropy data (most of the flux is composed of isotropized iron and heavy nuclei), as well as with the measured flux of extragalactic cosmic rays of energies above  $10^{18}$  eV. No new physics concerning the GZK cut-off mechanism is needed.

## Acknowledgment

The author is grateful to Arnold Wolfendale for valuable discussions and helpful comments.

## References

- [1] A.D. Erlykin and A.W. Wolfendale: “A single source of cosmic rays in the range  $10^{15}$  to  $10^{16}$  eV”, *Journal of Physics G*, Vol. 23, (1997), pp. 979–989.
- [2] A.D. Erlykin and A.W. Wolfendale: “Structure in the cosmic ray spectrum: an update”, *Journal of Physics G*, Vol. 27, (2001), pp. 1005–1030.
- [3] A.D. Erlykin and A.W. Wolfendale: “A search for ‘structure’ in the energy spectra of cosmic ray protons and He-nuclei above  $10^4$  GeV”, *Astroparticle Physics*, Vol. 10, (1999), pp. 69–81; “Supernova remnants and the origin of the cosmic radiation: I. SNR acceleration models and their predictions”, *Journal of Physics G*, Vol. 27, (2001) pp. 941–958; “Supernova remnants and the origin of the cosmic radiation: II. Spectral variations in space and time”, *Journal of Physics G*, Vol. 27, (2001), pp. 959–976; “Supernova remnants and the origin of the cosmic radiation: III. Spectral differences for different nuclei”, *Journal of Physics G*, Vol. 27, (2001), pp. 1709–1721.
- [4] T. Wibig and A.W. Wolfendale: “The anisotropy of arrival directions of cosmic rays above  $10^{17}$  eV”, *Journal of Physics G*, Vol. 25, (1999), pp. 2001–2009.
- [5] J. Szabelski, T. Wibig and A.W. Wolfendale: “Cosmic rays of the highest energies: the case for extragalactic heavy nuclei”, *Astroparticle Physics*, Vol. 17, (2002), pp. 125–131.
- [6] S.S. Al-Dargazelli, A.W. Wolfendale, A. Śmiałkowski and J. Wdowczyk: “The origin of cosmic rays of the highest energies”, *Journal of Physics G*, Vol. 22, (1996), pp. 1825–1838.
- [7] V. Berezhinsky: “Ultra high energy cosmic rays”, *Nuclear Physics Proc. Suppl.*, Vol. 70, (1999), pp. 419–430; “Ultra High Energy Cosmic Rays”, *Nuclear Physics Proc. Suppl.*, Vol. 81, (2000), pp. 311–322; “Ultra high energy cosmic rays from cosmological relics”, *Nuclear Physics Proc. Suppl.*, Vol. 87, (2000), pp. 387–396.
- [8] T. Wibig and A.W. Wolfendale: “The mass composition of cosmic rays above  $10^{17}$  eV”, *Journal of Physics G*, Vol. 25, (1999), pp. 1099–1112.
- [9] K. Greisen: “End to the cosmic ray spectrum?”, *Physical Review Letters*, Vol. 16, (1966), pp. 748–750.
- [10] G.T. Zatsepin and V.A. Kuzmin: “Upper limit of the spectrum of cosmic rays”, *Journal of Experimental and Theoretical Physics Letters*, Vol. 4, (1966), pp. 78–80.
- [11] M. Takeda et al.: “Extension of the cosmic ray energy spectrum beyond the predicted Greisen-Zatsepin-Kuz’min cutoff”, *Physical Review Letters*, Vol. 81, (1998), pp. 1163–1166.
- [12] C. Isola and G. Sigl: “Large scale magnetic fields and the number of cosmic ray sources above  $10^{19}$  eV”, *Physical Review D*, Vol. 66, (2002), p. 083002.
- [13] G. Bertone, C. Isola, M. Lemoine and G. Sigl: “Ultrahigh-energy heavy nuclei propagation in extragalactic magnetic fields”, *Physical Review D*, Vol. 66, (2002), p. 103003.
- [14] P.P. Kronberg: “Extragalactic magnetic fields”, *Reports on Progress in Physics*, Vol. 57, (1994), pp. 325–382.
- [15] D. Harari, S. Mollerach, E. Roulet and F. Sanchez: “Lensing of Ultrahigh-energy cosmic rays in turbulent magnetic fields”, *Journal of High Energy Physics*, (2002), 0203:045,2002; M. Bossa, S. Mollerach and E. Roulet: “Decaying neutron



- propagation in the Galaxy and the cosmic ray anisotropy at 1 EeV”, *Journal of Physics G*, Vol. 29, (2003), pp. 1409–1422.
- [16] T. Wibig and A.W. Wolfendale: “Ultra-high energy cosmic rays from transient extragalactic sources”, *Journal of Physics G*, Vol. 30, (2004), pp. 525–542.
- [17] M.A. Malkan and F.W. Stecker: “An empirically based calculation of the extragalactic infrared background”, *Astrophysical Journal*, Vol. 496, (1998), pp. 13–16.
- [18] M. Takeda et al.: “Small-scale anisotropy of cosmic rays above  $10^{19}$  eV observed with the Akeno Giant Air Shower Array”, *Astrophysical Journal*, Vol. 522, (1999), pp. 225–237.
- [19] F.W. Stecker and M.M. Salamon: “Photodisintegration of ultrahigh-energy cosmic rays: a new determination”, *Astrophysical Journal*, Vol. 512, (1999), pp. 521–526.
- [20] P. Lipa: “On the measurement of correlations and intermittency”, In: R.C. Hwa (Ed.): *Fluctuations and Fractal Structure*, Proc. of Ringberg Workshop, World Scientific, Singapore, (1992), pp. 96–110; P. Lipa, P. Currythers, H.C. Eggers and B. Buschbeck: “The correlation integral as probe of multiparticle correlations”, *Physics Letters B*, Vol. 285, (1992), pp. 300–308; “Integral correlation measures for multiparticle physics”, *Physical Review D*, Vol. 48, (1993), pp. 2040–2053; H.C. Eggers and P. Lipa: “Star integral and unbiased estimators”, Regensburg preprint TPR-93-25, <http://arxiv.org/hep-ph/9309256>.
- [21] M. Teshima et al.: “The Arrival Direction Distribution of Extremely High Energy Cosmic Rays Observed by AGASA”, Proceedings of the 28<sup>th</sup> International Cosmic Ray Conference, Tsukuba, (2003), pp. 437–440; J. Belz et al. for the HiRes Collaboration: “Anisotropy Studies of Ultra-High Energy Cosmic Rays Using Monocular Data Collected by the High-Resolution Fly’s Eye (HiRes)”, *ibid.*, (2003), pp. 425–428; C.B. Finley and S. Westerhoff for the HiRes Collaboration: “Small-Scale Anisotropy Studies of the Highest Energy Cosmic Rays Observed in Stereo by HiRes”, *ibid.*, (2003), pp. 433–436.
- [22] M. Takeda et al.: “Energy Determination in the Akeno Giant Air Shower Array Experiment”, Proceedings of the 28<sup>th</sup> International Cosmic Ray Conference, Tsukuba, (2003), pp. 381–384; D.R. Bergman for the High Resolution Fly’s Eye Collaboration: “Measurement of the Flux of UHE Cosmic Rays by the HiRes Detectors Observing in Monocular Mode”, *ibid.*, (2003) pp. 397–400; R.W. Springer for the High Resolution Fly’s Eye Collaboration: “Measurement of the Flux of UHE Cosmic Rays by the HiRes Detectors Observing in Both Monocular and Stereoscopic Modes”: *ibid.*, (2003), pp. 413–416; D. De Marco, P. Blasi and A.V. Olinto: “The GZK Feature in the Spectrum of UHECRs: What Is It Telling Us?”, *ibid.*, (2003), pp. 655–658.